

Parameters Optimization Development on Relative Density and Compression Strength of AlSi10Mg Sample Produced by Selective Laser Melting using Response Surface Method.

M S Wahab¹*, A A Raus², M.Ibrahim³, K Kamarudin⁴, Ahmed Aqeel⁵, E Z Radzi⁶, I M Amir⁷

¹ Faculty of Mechanical and Manufacturing Engineering, Universiti Tun Hussein Onn Malaysia, Batu Pahat, Johor, Malaysia.

² Centres for Instructor and Advanced Skill Training (CIAS), 40900 Shah Alam, Malaysia.

*Corresponding author E-mail: saidin@uthm.edu.my

Abstract

This paper investigates the effect of main process parameters such as laser power, scanning speed and hatching distance of selective laser melting process via relative density and compression strength using response surface method. Central composite design with three factor and three level has been used to develop the mathematical models on the relative density and compression strength of AlSi10Mg samples. The maximum and minimum relative density value recorded from the experiment measurement were 99.4785% and 97.2807% which occurred at design level 16 and 2. Meanwhile the maximum and minimum value of compression strength recorded were 545.578 MPa and 456.432 MPa which occurred at design level 15 and 2. The adequacy of the suggested mathematical models were verified from the analysis of variance (ANOVA) method and used to determine the optimized results. The optimized results on relative density and compression strength from Design Expert software were 99.3547 % and 545.578MPa, respectively occurred at 348.14 watt of laser power, 1483.25 mm/s scan speed and 0.1207 mm hatch distance. The optimized parameters were confirmed with three fabricated samples with an average value of 98.1123 % relative density and 540.597 MPa. These values were within 95% confidence level and evidenced that the developed models were adequate for both experiments.

Keywords: AlSi10Mg; Compression Strength; Relative Density; Response Surface Method; Selective Laser Melting.

1. Introduction

Almost more than three decade additive manufacturing (AM) has been introduced and used to fabricate complex design product which normally cannot be fabricated by conventional machining due to the trend of customization demand. Among of the AM technological approaches from layer manufacturing (LM) technological methods such as direct metal laser fabrication (DLMF), electron beam melting (EBM) and selective laser melting (SLM) were the dominant AM technological approaches which able to fabricate metal part by a single step process referring to the 2-D cross sections from the 3D design generated from Computer Aided Design (CAD). Medical and dental industry are concentrating on the SLM using Ti-6Al-4V and Co-Cr-Mo alloys to acquire the mechanical and chemical properties as well as accuracy and geometrical feasibility to ensure the SLM produced part satisfy the requirements for medical or dental parts [1]. While, Miguel Seabra et al [2] focused on the combination of topology optimization (TO) and SLM using Ti-6Al-4V alloy in the aerospace industry. The experimental result revealed that with the combination of TO and SLM to fabricate part with an optimize amount of Ti-6Al-4V powder distribution will increase the mechanical strength despite reduction in part weight. Noriko Read et al [3] has investigated the effect of SLM main processing parameters on porosity using statistical method. A set of optimized SLM main processing parameters were obtained base on minimal porosity. The optimum SLM main processing parameters were validated through creep mechanical testing and revealed a better strength and elongation properties compared to high pressure die cast alloy with the similar composition.

The SLM fabrication is influenced by numerous of parameters which has a specific effect on the part quality. However the principal parameters which influenced the quality of the sample and usually been investigated by researchers are related to laser power, scanning speed and hatching distance [4]. The energy density is determined by laser power (LP), scan speed (SS), hatch distance (HD) and layer thickness (LT) by the following equation. Whereby the selection building chamber atmosphere and scanning pattern during the fabrication process will also enhance the part quality. Recently, many experiments and study works were conducted regarding the properties of laser sintered samples using mentioned parameters to increase the qualities and suit the functional of the customized products using different type of materials[4]-[7].

$$\text{Energy Density, } E_d = \left(\frac{P_l}{v * h * t} \right) \quad (1)$$

Where; P_l = laser power (watt); v = Scan Speed (mm/s); h = hatch distance (mm); t = layer thickness (mm)

The beneficial of design of experiment (DOE) and statistical approaches frequently has been used to investigate the influence of main processing parameters in AM during fabricating various type of material. By using the analysis of variance (ANOVA), it will performed further analysis between the input parameters and the corresponding responses and generate a mathematical model that represent the correlation factor. Optimization on the parameters to produce the expected output can also been completed during this analyses. Noriko Read et al [3] investigated the optimization parameters process to reduce porosity during the fabrication the AlSi10Mg sample using SLM. The optimum parameters were used to fabricate samples for examined the creep properties. The researchers found that the SLM produced samples exhibited higher strength and elongation properties compared to die cast Al alloys with similar type. Luke N. Carter [8] used the DOE techniques and ANOVA analysis to investigate the effect of SLM process parameters for producing a free void sample. The researcher found out that the energy density can be optimized to eliminate large voids, however, the formations of cracks during the fabrication process has no correlation.

The main objective of this paper is to investigate the effect of the main SLM parameters on relative density (RD) and compression strength (CS) of AlSi10Mg sample. Response surface method (RSM) and variance analysis (ANOVA) will be used to optimize the parameters and developing the mathematical models. Furthermore, the models will be used to predict to value of relative density and compression strength and recommended the optimized parameters to maximize these properties. The motivation of this experiment is to compare the optimized compression result with the same of the generally used high pressure die cast A360 alloy.

2. Experiment work

In this research project, AlSi10Mg powder supplied from LPW Technology Ltd was used to fabricate to samples. The SLM 280 HL machine was engaged to fabricate the samples. The machine system is equipped with a $280 \times 280 \times 350$ mm building chamber, a 400 W fiber laser with $80 \mu\text{m}$ laser beam spot. The build chamber is filled with Argon gas to prevent oxidization. In order to reduce internal stress in the component the assembly platform is heated up to over 150°C during the process. The aluminium substrate plate is mounted on top of the building platform and levelled. The compression test was carried out in a Testometric M500 testing machine applying the cross-head speed of 1.00 mm/min, as shown in Figure 1, following the ISO 6892 and ASTM E 9 – 89a standards. The latter standard was particularly for the geometry of the compression specimen. These specimens were of cylindrical shape having the diameter of 13 mm and overall length of 25 mm. The approximate ratio between the length and diameter was 2.0. Figure 2 shows the samples built by the SLM process.

3. Design of experiment

3.1. Response surface methodology

The response surface methodology (RSM) was developed by Box and Wilson in 1951. It is one of many statistical and mathematical techniques for creating design of experiments, assessing the effect of independent variables on dependent output, developing models and processes optimization. The vital capabilities of RSM is to develop the functional relationship of output (Y) and the independent variables. Once all the independent variables are controllable and measureable in the designed experiment, the response surface can be describe as a liner function and can be described by the following equation:

$$Y = \beta_0 + \beta_1 X_1 + \beta_2 X_2 + \dots + \beta_k X_k + \varepsilon \quad (2)$$

Where $X_1, X_2 \dots, X_k$ are the independent variables, β_0 is the constant coefficient, β_k is the linear of the n th factor coefficient and ε is the error observed.

Frequently a second order polynomial, as a quadratic function as is employed in RSM and can be described by the following equation:

$$Y = \beta_0 + \sum_{i=1}^k \beta_i X_i + \sum_{i=1}^k \beta_{ii} X_i^2 + \dots + \sum_{i < j} \beta_{ij} X_i X_j + \varepsilon \quad (3)$$

Where β_{ii} expresses the quadratic effect of the i th factor and β_{ij} displays the effect of interaction between the i th and j th factors.



Fig. 1: Testometric M500 compression testing machine



Fig. 2: The compression samples built by the SLM process.

3.2. Central composite design

Central composite design (CCD) was selected in this experiment, which is the most popular and efficient tool in RSM. In this study Design Expert version 10 was used to analyse the results and data processing by using α value is 1.68179, rotatable with six centre points. Table 1 shows the actual value and levels of the design parameters. The CCD consisted of totally 20 experiments with the independent variable of laser power, scan speed and hatch distance. Table 2 displays the created design of experiment and the corresponding results of RD and CS for each experiment.

Table 1: Processing parameters range and level of SLM

Machine parameter	Unit	Level		$\alpha = 1.68179$	
		Low	High	+ α	- α
LP	Watt	320	380	299.546	400.454
SS	mm/s	1150	1750	945.462	1954.54
HD	mm	0.1	0.15	0.083	0.167

Table 2: Design of experiment and the corresponding results of relative density and compress strength

Experiment no.	Machine parameter			Response	
	LP (Watt)	SS (mm/s)	HD (mm)	RD (%)	CS (MPa)
1	-1.000	-1.000	-1.000	98.541	480.094
2	1.000	-1.000	-1.000	97.2807	456.432
3	-1.000	1.000	-1.000	97.6705	497.341
4	1.000	1.000	-1.000	98.7229	489.822
5	-1.000	-1.000	1.000	98.075	480.493
6	1.000	-1.000	1.000	96.6044	464.689
7	-1.000	1.000	1.000	96.5039	461.703
8	1.000	1.000	1.000	97.5968	479.578
9	-1.682	0.000	0.000	98.5091	486.246
10	1.682	0.000	0.000	97.9481	480.945
11	0.000	-1.682	0.000	97.7968	476.578
12	0.000	1.682	0.000	98.0245	499.38
13	0.000	0.000	-1.680	97.4902	477.066
14	0.000	0.000	1.680	96.2615	463.564
15	0.000	0.000	0.000	99.1327	545.578
16	0.000	0.000	0.000	99.4785	542.545
17	0.000	0.000	0.000	99.2497	544.51
18	0.000	0.000	0.000	99.3128	540.789
19	0.000	0.000	0.000	99.3698	542.879
20	0.000	0.000	0.000	99.325	543.989

4. Result and discussion

4.1. Mathematical models development

The influence of the independent factors on the corresponded responses of the regression models were examined at confidence level of 95% ($\alpha=0.05$) using Design Expert software version 10. The second order polynomial equation or the quadratic equation model was designated to predict the corresponded responses. The final regression equation models for RD and CS are stated in equations (3) and (4). A, B and C represented the independent factors of Laser Power, Scan Speed and Hatch Distance, respectively.

$$RD = 99.31 - 0.11*A + 0.028*B - 0.40*C + 0.61*AB - 0.021*AC - 0.14*BC - 0.37*A^2 - 0.48*B^2 - 0.85*C^2 \quad (3)$$

$$CS = 543.40 - 2.78*A + 6.23*B - 4.39*C + 6.23*AB + 4.16*AC - 6.82*BC - 21.24*A^2 - 19.69*B^2 - 25.99*C^2 \quad (4)$$

4.2 Adequacy of the developed models

The variance analysis (ANOVA) was done to check developed models and at this stage the significance of the proposed models was measured to predict the corresponded responses. The ANOVA for RD and CS, using the second order polynomial as a quadratic function

are shown in Tables 3 and 4. Both the results reveal that all the models are statistically significant since the p value is less than 0.05. The determination coefficient (R^2) is another method to calculate the developed model's accuracy in forecasting the corresponded responses. If the value is closer to unity, then the predicted results can be more accurate. In the experiment of RD and CS, the determination coefficient (R^2) values were 0.9926 and 0.9964, respectively indicating that the model was adequate in representing the experimental results. Meanwhile, the signal to noise ratio was measured by adequate precision value and the required value was more than 4. Both relative density and CS indicated an adequate signal with the values of 36.498 and 46.87, respectively

Table 3: Analysis of variance (ANOVA) for the RD

Source	Sum of Squares	df	Mean Square	F- Value	p-value Prob > F
Model	19.21	9	2.13	149.80	< 0.0001
A-laser Power	0.17	1	0.17	12.02	0.0061
B-Scan Speed	0.010	1	0.010	0.73	0.4140
C-Hatch Distance	2.22	1	2.22	155.58	< 0.0001
AB	2.97	1	2.97	208.63	< 0.0001
BC	0.17	1	0.17	11.61	0.0067
A ²	1.99	1	1.99	139.58	< 0.0001
B ²	3.37	1	3.37	236.85	< 0.0001
C ²	10.41	1	10.41	731.01	< 0.0001
Residual	0.14	10	0.014		
Lack of Fit	0.075	5	0.015	1.12	0.4528
Pure Error	0.067	5	0.013		
Cor Total	19.35	19			
Std. Dev.	0.12		R-Squared	0.9926	
Mean	98.14		Adj R-Squared	0.9860	
C.V. %	0.12		Pred R-Squared	0.9649	
PRESS	0.68		Adeq Precision	36.498	

Table 4: Analysis of variance (ANOVA) for the CS

Source	Sum of Squares	df	Mean Square	F- Value	p-value Prob > F
Model	20000.43	9	2222.27	309.86	< 0.0001
A-laser Power	105.87	1	105.87	14.76	0.0033
B-Scan Speed	530.09	1	530.09	73.91	< 0.0001
C-Hatch Distance	263.04	1	263.04	36.68	0.0001
AB	310.28	1	310.28	43.26	< 0.0001
AC	138.21	1	138.21	19.27	0.0014
BC	371.80	1	371.80	51.84	< 0.0001
A ²	6503.84	1	6503.84	906.8	< 0.0001
B ²	5589.46	1	5589.46	779.3	< 0.0001
C ²	9704.74	1	9704.74	1353.	< 0.0001
Residual	71.72	10	7.17		
Lack of Fit	57.58	5	11.52	4.07	0.0747
Pure Error	14.14	5	2.83		
Std. Dev.	2.68		R-Squared	0.996	
Mean	497.71		Adj R-Squared	0.993	
C.V. %	0.54		Pred R-Squared	0.974	
PRESS	518.47		Adeq Precision	46.87	

Additionally, the normal probability plot of residuals graphs along with the predicted vs. actual values graphs were generated from the results of ANOVA. The residuals graphs' normal probability plot is displayed in Figure 3 and 4. The plotted graphs determined the suitability of the collected corresponded response values in the distribution line. The closer corresponded response values plotted in the distribution line was responsible for better fitness of the designated distribution. Although both graphs show all the points laid near the line but the CS points are fitted closer to the distribution line. Hence, a better value was provided in the normal probability plot of residuals compared to the RD values. The predicted vs. actual values graphs are shown in Figure 5 and 6. These graphs that explain the quality of correlation between the actual and the predicted values of the developed model, indicate a good correlation in this case.

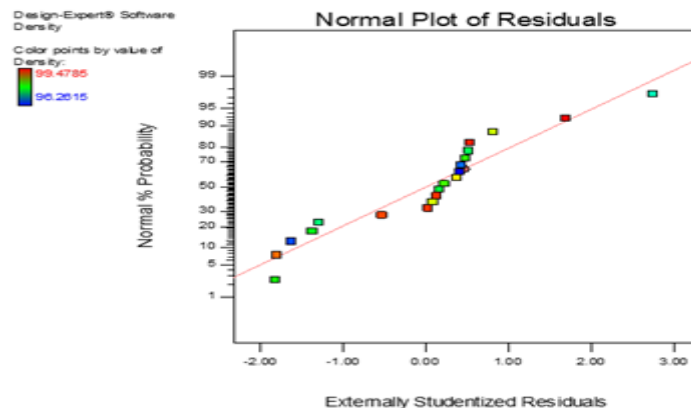


Fig. 3: Normal plot of residuals for RD

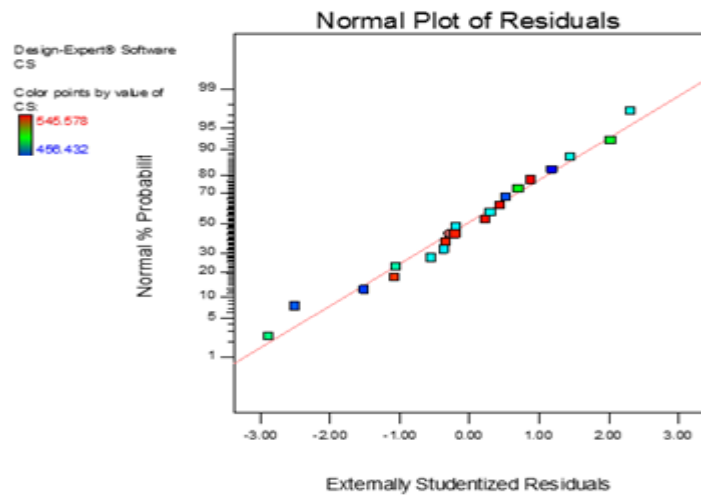


Fig. 4: Normal plot of residuals for CS

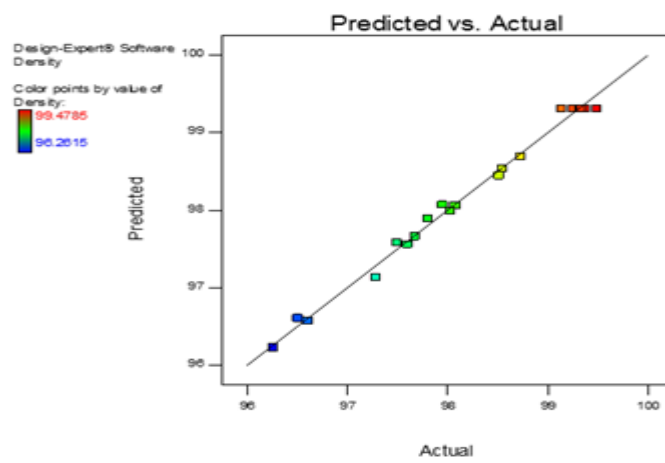


Fig. 5: Predicted vs. actual for RD

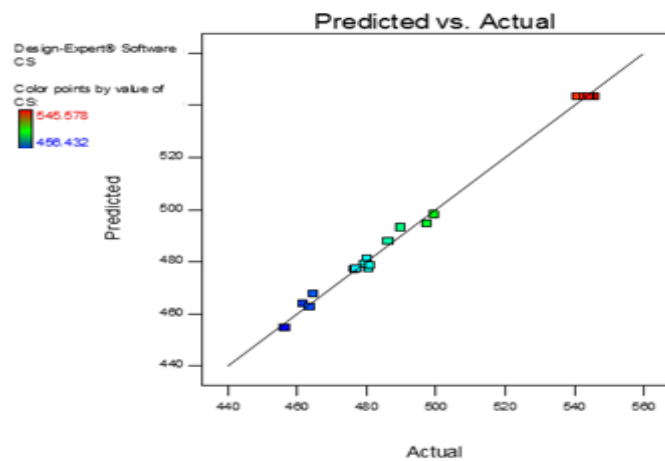


Fig. 6: Predicted vs. actual for CS

4.3 Response surface analysis for relative density

The response surface graphs and counter plots analysis were used to determine and visualize the influence of independent factors on the corresponded responses based on the regression equation models. The optimal response can be identified from the 3D response surface graphs. Figures 7, 8 and 9 display the 3D response surface graph and contour plot that represents the parameters' influence on the RD. Figure 5 reveals the effect of scan speed and laser power on the relative density by keeping the hatch distance constant at 0.125 mm (zero level). It can be analyzed from the graphs that the relative density decreases with the increasing value of scan speed and laser power, where the latter has slightly greater effect on the response. Figure 7 displays the impact of hatch distance and laser power at constant scan speed for zero level. The graph shows that the maximum relative density can be determined at almost zero level of input parameters. Whereas, both parameters can identify that the relative density is at lowest value at the maximum and minimum magnitude of these pa-

rameters. Figure 8 represents the influence of hatch distance and scan speed when the laser power is at zero level. The trend of the response surface graphs was almost identical with the Figure 9. However, it can be observed that the highest value of the relative density reaches almost zero level for hatch distances and passes zero level for scan speed. The 3D response surface graphs and contour plots analysis in Figures 7, 8 and 9 illustrates that the maximum relative density of the SLM produced part is 99.4785 %. The outcomes from these graphs are in close agreement with numbers of previous research work [9], [10] explained that the RD are strongly influenced by laser power, scan speed and hatch speed.

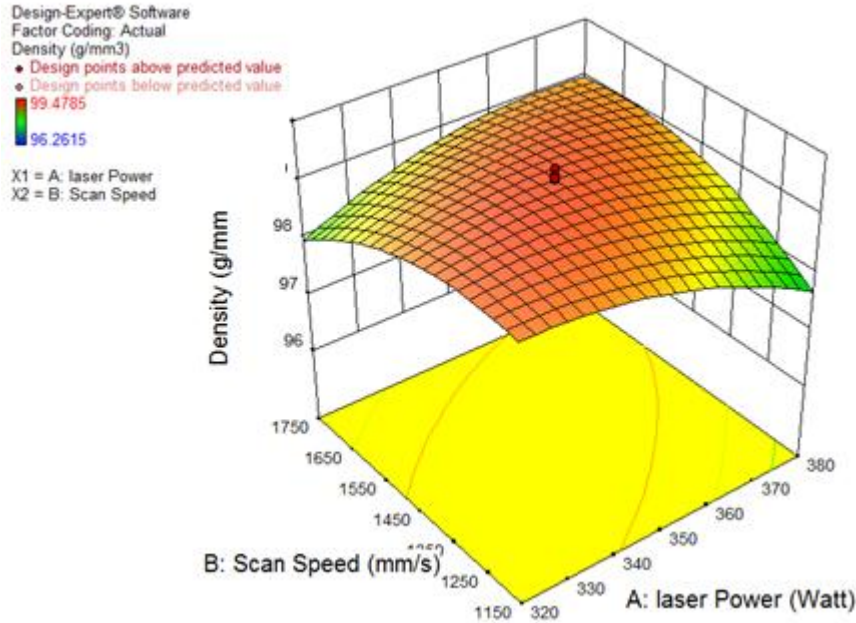


Fig. 7: 3D surface RD vs. laser power and scan speed

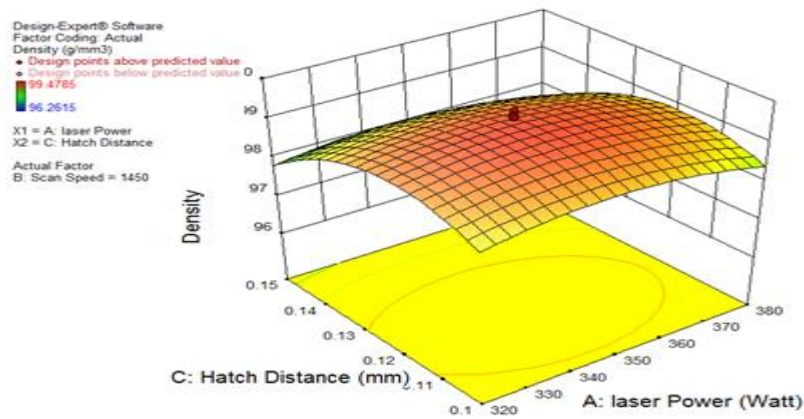


Fig. 8: 3D surface RD vs. laser power and hatch distance

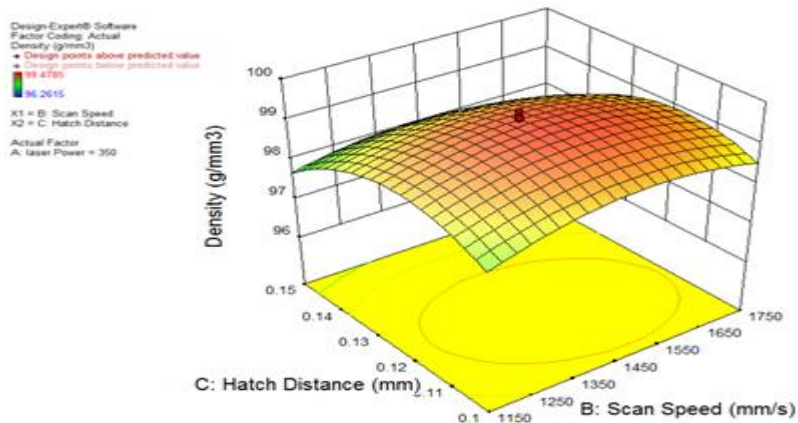


Fig. 9: 3D surface RD vs. scan speed and hatch distance

4.4.4 Response surface analysis for compression strength

Figures 10, 11 and 12 display the response surface graphs and counter plots to show the SLM input parameter's effect on CS. Figure 10 illustrates the correlation between the scan speed and the laser power keeping the input hatching distance constant at zero level. The CS was at the lower value for the maximum input of scan speed and laser power. The CS increased with the increasing laser power until it reached the zero level and dropped to the lowest value when the laser power was at maximum level. The maximum value of CS was obtained within the range of 1450 - 1650 mm/s for scan speed and 340 - 360 watt for laser power. Figure 11 exhibits the effect of hatching distance and laser power with constant scan speed at zero level. The response surface graphs and counter plots almost attained the bull's eye condition and the obtained maximum value of CS was located almost at the zero level for all the input parameters. Figure 12 describes the influence of scan speed and hatch distance while the laser power was held at zero level. The CS value was increased with the increasing value of scan speed and attained the highest value at the maximum level of scan speed. It was also found that the maximum and minimum level of hatch distance contributed to the negative impact of CS value. Through the 3D response surface graphs and contour plots analysis as per Figures 10 to 12, the highest value of CS for the part, produced by SLM, was 545.578 MPa.

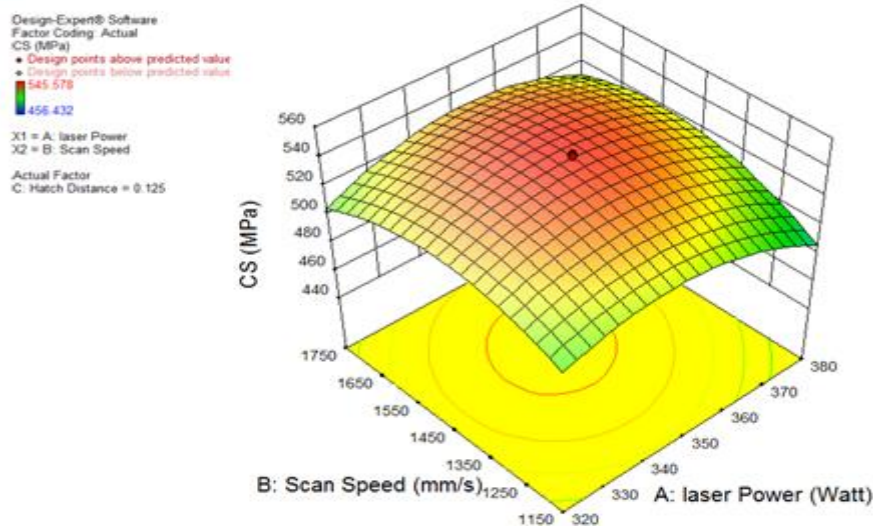


Fig. 10: 3D surface CS vs. laser power and scan speed

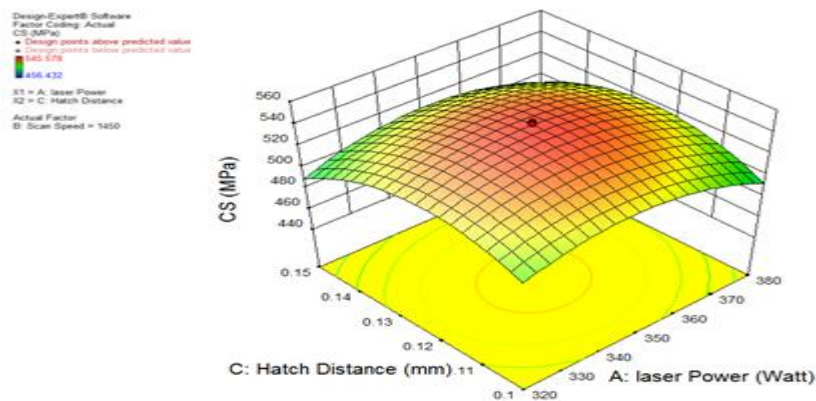


Fig. 11: 3D surface CS vs. laser power and hatch distance

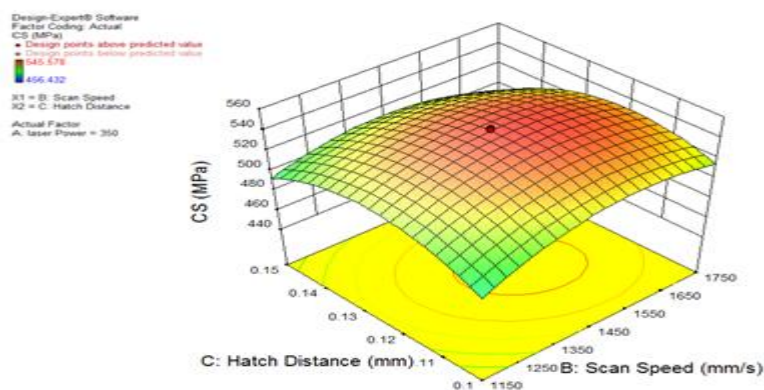


Fig. 12: 3D surface and CS vs. scan speed and hatch distance

4.5 Optimization on SLM parameters

The analysis was completed using the optimization response module of Design Expert software at the optimization stage for RD and CS. Although the achieved maximum values of RD and CS from the experiments were 99.4785 % and 545.587 MPa respectively, but the software indicated their values that were accomplished by the optimized SLM parameters were 99.3547 % and 544.057 MPa respectively. The optimized SLM parameters to achieve the maximum relative density and CS are tabulated in Table 5. The outcomes from this experiment are in close agreement with the numbers of previous research works [11], [12] and they acknowledged that CS was proportionally affected by the RD.

Table 5: Optimum SLM parameters values against RD and CS

Optimized SLM Parameters			Response Output	
Laser Power (Watt)	Scan Speed (mm/s)	Hatch Distance (mm)	Relative Density (%)	Ultimate Compressive Strength (MPa)
348.14	1483.25	0.1207	99.3547	545.578

Three specimens were fabricated based on the optimized SLM parameters and test were conducted to verify the regression models. The confirmation test were conducted not only using the optimized parameters that achieved maximum output but also conducted using the parameters that will produced the minimum result of RD and CS. Table 6 shows the predicted and conducted experiment values, which possess an acceptable error within 95% confidence level and evidenced that the developed models were adequate for both experiments. The compression samples reached their tensile limit due to the fracture under the compressive force up to 100 kN as displayed in Figure 13. The compressive yield strength of the compression sample was outperformed when compared with the same of the generally used high pressure die cast A360 alloy which possessed a value of 100 Mpa. The finer microstructure of the compression sample produced by SLM was the major reason that attributed to the higher compressive yield strength.

Table 6: Validation of optimization results

SLM Parameters	Response Output	Experiment value(Avg.)	Predicted Value	Error (%)
LP-348.14 W	RD (%)	98.1123	99.3547	1.18
SS- 1483.25 mm/s	CS (Mpa)	540.597	545.578	0.91
HD-0.1207 mm	RD (%)	96.185	97.8689	1.72
LP-371.815 W	CS (Mpa)	478.685	483.916	1.08
SS-1150.02 mm/s				
HD- 0.108 mm				



Fig. 13: Compression samples before and after testing

The compressive strength values were also outperformed when compared with the value of tensile strength from previous research works [9], [11], [13] due to the minimal effect of porosity in the compression test. Only when the porosity was nominal, the nature of loading in the compression test tried to consolidate the defected areas by closing the pores. Meanwhile, the pores were stretched under tensile loading and it initiated the cracks leading to the failure. Due to the minimal effect of porosity, the defect in the compressive loading motivated the application of SLM to fabricate the plastic injection moulding tools.

5. Conclusion

In this experiment study, RD and ultimate CS of AlSi10Mg sample produced by Selective Laser Melting has been investigated using statistical method. Response Surface Method specifically central composite design approach was used to develop the correlation relationship between the input parameters and the corresponding responses. Confirmation tests were conducted to verify the equation regression models within the confidence level of 95%. The conclusions can be drawn from this experiment study are as follows:

- The mathematical models was successfully developed using RSM with central composite design was to predict the RD and CS of the AlSi10Mg sample fabricated by SLM.
- The ANOVA analyses shows that both mathematical models was highly significant. Laser power and hatch distance were the most significant factors that contributed to the maximum value of relative density, meanwhile scan speed was categorized not significant due to the P value (0.414) is greater than the α value (0.05). However laser power, scan speed and hatch distance were categorized as the highly significant factor that contributed to the achievement of maximum value of CS due to the lower P value compared to the α value (0.05).

- The optimum values input parameters for laser power, scan speed and hatch distance recommended to achieve maximum value of RD and CS were 348.14 Watt, 1483.25 mm/s and 0.1207 mm, respectively. The recommended results by the software were in line to default parameters suggested by the machine manufacture for part fabrication using AlSi10Mg.
- Other than almost full density achievement with the value of 99.3547% from the experiment, the experimental value of CS (545.587 MPa) was higher compared to A360F and A360T6 HDPC alloys. It also can be concluded that the produced part from SLM technique possessed superior physical and mechanical properties, however with further investigation of SLM parameters will enhanced the properties depending on the functionality of the desire part.

Acknowledgement

This research work is financially supported by Research Innovation Commercialization and Consultancy Management (ORICC) and Centre for Graduate Studies (CGS), University Tun Hussein Onn Malaysia (UTHM).

References

- [1] B. Vandenbroucke and J. Kruth, "Selective laser melting of biocompatible metals for rapid manufacturing of medical parts," *Rapid Prototyp. J.*, vol. 13, no. 4, pp. 196–203, 2007.
- [2] M. Seabra, J. Azevedo, A. Araújo, L. Reis, E. Pinto, N. Alves, R. Santos, and J. Pedro Mortágua, "Selective laser melting (SLM) and topology optimization for lighter aerospace components," *Procedia Struct. Integr.*, vol. 1, pp. 289–296, 2016.
- [3] N. Read, W. Wang, K. Essa, and M. M. Attallah, "Selective laser melting of AlSi10Mg alloy: Process optimisation and mechanical properties development," *Mater. Des.*, vol. 65, pp. 417–424, 2015.
- [4] N. T. Aboulkhair, N. M. Everitt, I. Ashcroft, and C. Tuck, "Reducing porosity in AlSi10Mg parts processed by selective laser melting," *Addit. Manuf.*, vol. 1–4, pp. 77–86, 2014.
- [5] D. Manfredi, F. Calignano, M. Krishnan, R. Canali, E. P. Ambrosio, and E. Atzeni, "From powders to dense metal parts: Characterization of a commercial alsiing alloy processed through direct metal laser sintering," *Materials (Basel)*, vol. 6, no. 3, pp. 856–869, 2013.
- [6] M. Krishnan, E. Atzeni, R. Canali, D. Manfredi, F. Calignano, E. P. Ambrosio, and L. Iuliano, "On the effect of process parameters on properties of AlSi10Mg parts produced by DMLS," *Rapid Prototyp. J.*, p. manuscript accepted, 2014.
- [7] N. Raghunath and P. M. Pandey, "Improving accuracy through shrinkage modelling by using Taguchi method in selective laser sintering," *Int. J. Mach. Tools Manuf.*, vol. 47, no. 6, pp. 985–995, 2007.
- [8] L. N. Carter, K. Essa, and M. M. Attallah, "Optimisation of selective laser melting for a high temperature Ni-superalloy," *Rapid Prototyp. J.*, vol. 21, no. 4, pp. 423–432, 2015.
- [9] R. A.A, W. M.S, I. M., K. K., A. Ahmed, and S. S, "Mechanical and Physical Properties of AlSi10Mg Processed through Selective Laser Melting," *Int. J. Eng. Technol.*, vol. 8, no. 6, pp. 2612–2618, 2016.
- [10] A. A. Raus, M. S. Wahab, Z. Shayfull, K. Kamarudin, M. Ibrahim, M. M. A. B. Abdullah, S. Z. Abd Rahim, M. F. Ghazali, N. Mat Saad, M. M. Ramli, S. A. Zainol Murad, S. S. Mat Isa, and S. Sharif, "The Influence of Selective Laser Melting Parameters on Density and Mechanical Properties of AlSi10Mg," *MATEC Web Conf.*, vol. 78, p. 1078, 2016.
- [11] N. T. Aboulkhair, "Additive manufacture of an aluminium alloy : processing , microstructure , and mechanical properties," no. December, 2015.
- [12] P. George and E. Jerrard, "Selective Laser Melting of Advanced Metal Alloys for Aerospace Applications," 2011.
- [13] K. Kempen, L. Thijs, J. Van Humbeeck, and J.-P. Kruth, "Processing AlSi10Mg by selective laser melting: parameter optimisation and material characterisation," *Mater. Sci. Technol.*, vol. 31, no. 8, pp. 917–923, 2015.